Supplementary Information for:

Human monoclonal antibodies that target clade 2.3.4.4b H5N1 hemagglutinin

Garazi Peña Alzua[1,2], André Nicolás León[3], Temima Yellin[1,2], Disha Bhavsar[1,2], Madhumathi Loganathan[1,2], Kaitlyn Bushfield[1,2], Philip J.M. Brouwer[3], Alesandra J. Rodriguez[3], Trushar Jeevan[4], Richard Webby[4], Christine Marizzi[1,5,6], Julianna Han[3], Andrew B. Ward[3], J. Andrew Duty[1,7*] and Florian Krammer[1,2,6,8,9*]

[1]Department of Microbiology, Icahn School of Medicine at Mount Sinai, New York, NY, USA
[2]Center for Vaccine Research and Pandemic Preparedness (C-VaRPP), Icahn School of Medicine at Mount Sinai, New York, NY, USA
[3]Department of Integrative Structural and Computational Biology, The Scripps Research Institute, La Jolla, CA, USA
[4]Department of Host Microbe Interactions, St Jude Children's Research Hospital, Memphis, TN, USA
[5]BioBus, New York, NY, USA
[6]Ludwig Boltzmann Institute for Science Outreach and Pandemic Preparedness at the Medical University of Vienna, Vienna, Austria
[7]Center for Therapeutic Antibody Development, Icahn School of Medicine at Mount Sinai, New York, NY, USA
[8]Department of Pathology, Molecular and Cell Based Medicine, Icahn School of Medicine at Mount Sinai, New York, NY, USA
[9]Ignaz Semmelweis Institute, Interuniversity Institute for Infection Research, Medical University of Vienna, Vienna, Austria

*To whom correspondence should be addressed: andrew.duty@mssm.edu and florian.krammer@mssm.edu

Supplementary Methods

Cells. Madin-Darby canine kidney (MDCK) cells (ATCC #CCL-34) were passaged and cultured in Dulbecco's modified Eagles medium (DMEM, Gibco) supplemented with 10% fetal bovine serum (FBS, Gibco) penicillin (100U/ml) and streptomycin (100ug/ml) (P/S) at 37°C and 5% CO_2. MDCK cells were used for *in vitro* microneutralization assays. Expi293F cells were maintained in Expi293 Expression Medium in a shaking incubator at 37°C and 8% CO2. Expi293F cells were used for monoclonal antibody (mAb) production.

Recombinant glycoproteins. HA proteins (as soluble trimers) and NA proteins (as soluble tetramers) were expressed from various virus strains, including H5N1 strains from birds and mammals, including humans. HA proteins used in this study are referred to with the use of GISAID numbers and GenBank numbers: HA was used as an antigen; A/mallard/New York/22-008760-007-original/2022 (H5) (GISAID number EPI2017135). HA protein of viruses isolated from New York Virus Hunters community science initiative (NYCVH)[1,2] includes: A/chicken/New York/NYCVH 168127/2023 (H5N1) (GenBank number WPF52968.1), A/Canada goose/New York/NYCVH 23-453/2023 (H5N1) (GenBank number WPL83443.1), A/Canada goose/New

York/NYCVH 22-9190/2022 (H5N1) (GenBank number WPF48542.1), A/peregrine falcon/New York/NYCVH 160820/2022 (H5N1) (GenBank number WPF49852.1), A/red-tailed hawk/New York/NYCVH 22-8477/2022 (H5N1) (GenBank number WPF47596.1). HA protein from the virus strain used to characterize the mAbs *in vitro*, A/bald eagle/FL/W22-134-OP/2022 (H5N1) (GISAID number EPI3661109). HA proteins from virus strains isolated from infected birds in 2014 include: A/chicken/Netherlands/14015531/2014 (H5N8) (GISAID number EPI2817295), A/Northern pintail/WA/40964/2014 (H5N1) (GenBank number AJE30344.1). HA protein from a virus isolated from infected dairy cattle: A/dairy cattle/Texas/24-008749-001-original/2024 (GISAID number EPI3158678). HA proteins from virus strains isolated from infected humans: A/Vietnam/1203/2004 (H5N1) (GISAID number EPI1990181), A/Indonesia/5/2005 (H5N1) (GenBank number AFM78567.1), A/Shenzhen/1/2016 (H5N1) (GISAID number EPI687704), A/Cambodia/NPH230032_2/2023 (H5N1) (GISAID number EPI2419978), A/Wisconsin/67/2022 (H1N1) (GISAID number EPI2224788).

Immunization. Eight- to twelve-week-old H2L2 Harbour Mice® mice were immunized intraperitoneally with HA and NA from A/mallard/New York/22-008760-007-original/2022 (H5N1) adjuvanted with 40ug of poly I:C (InvivoGen, San Diego, CA). Each mouse received a prime followed by two boosts, and blood was collected two weeks after each boost to monitor the titer of serum antibodies via enzyme-linked immunosorbent assay (ELISA) and hemagglutination inhibition (HI) analysis. All experiments were performed according to protocols approved by the Icahn School of Medicine at Mount Sinai Institutional Animal Care and Use Committee (IACUC).

Concentration and purification of recombinant (r)mAbs in 293 suspension cells. After seven days of transfecting Expi293F cells with the DNA plasmid of the light and heavy chains and incubation in a shaking incubator at 37°C, supernatant containing IgG was first clarified by centrifugation at 4,000g for 30 minutes (min), sing 0.45uM Stericup filters (Sigma-Aldrich). The clarified supernatant was then purified using IgG-Fc packed columns (Thermo Scientific) by gravity flow, concentrated with Vivaspin 500 centrifugal concentrator, 30,000 molecular weight cut-off (MWCO) (GE Lifescience) and quantified with the nanodrop. The heavy and light chain plasmids of an irrelevant human IgG control monoclonal antibody were co-transfected and purified similarly.

ELISA. 96-well plates (Immulon 4 HBX; Thermo Scientific) were coated with 50ul of H5 recombinant protein (2ug/ml) and incubated at 4°C overnight. The next day, plates were blocked with 200ul/well of 3% non-fat milk in phosphate-buffered saline (PBS, Gibco) with 0.1% Tween (Fisher Scientific) (PBST) for 1hour (h) at room temperature (RT). After discarding the blocking solution, 100ul of serially diluted IgG, at a starting concentration of 30ug/ml in PBST-1% non-fat milk was added to the plates in duplicates for 2h at RT. Plates were washed three times with PBST, and mAbs binding was detected by a secondary horseradish peroxidase (HRP)-labeled anti-human IgG (GE Healthcare) diluted 1:3000 in PBST-1% non-fat milk, incubated for 1h at RT, followed by three PBST washes. 3,3′, 5,5′-tetramethylbenzidine (TMB, Thermo Scientific) was added for 10min, followed by Stop Solution (Invitrogen). Absorbance was determined at 450nm via a Synergy 4 (BioTek) plate reader. An anti-HA antibody, CR9114[3] was used as a positive control, while an anti-severe acute respiratory syndrome coronavirus 2 (SARS-CoV-2) spike antibody[4] was used as a negative control. Control wells contained only secondary antibody.

Virus production. 10-day-old embryonated chicken eggs (Charles River Laboratories) were inoculated with the virus and incubated at 37°C for 48h. Allantoic fluid was collected after the eggs were chilled at 4°C overnight and clarified by centrifugation at 3800 x g for 30min before freezing at -80°C.

Determination of virus HA titer. HA titer of the viruses was determined in allantoic fluid collected from infected eggs. In brief, the collected allantoic fluid was spin at 3,000g for 10min, supernatant was collected and serially diluted (1:2) in a V-bottom 96-well plate (ThermoFisher), testing each dilution in replicates. Turkey red blood cells (RBCs) were first washed and then suspended in PBS, at a concentration of 0.5%, and were added to the virus-containing plate. After 45min of incubation at 4°C, virus positive wells were visualized based on the formation of a pellet. No pellet indicates binding of hemagglutinin to the sialic acid receptors on RBCs and hence, lack of a pellet was considered positive.

***In vitro* microneutralization assay.** To test neutralization of A/bald eagle/FL/W22-134-OP/2022 (H5N1-A/PR/8/34 reassortant), here referred to as clade 2.3.4.4b (H5N1-PR8) virus with human IgG**,** mAbs were serially diluted at a starting concentration of 25ug/ml in infection media (1xMEM with tosyl phenylalanyl chloromethyl ketone(TPCK)-treated trypsin), 100 times $3.82x10^4$ $TCID_{50}$/50ul of the virus was then added, and the mix was incubated in 100ul for 1h at RT, testing each antibody in duplicate. Virus-only controls were prepared by mixing virus with infection media. Virus-antibody mixes, virus-only mixes, or medium-only were then added to MDCK cells seeded at 25000cells/well in 96-well plates (Corning) the day prior. Following 1h incubation, cells were washed with PBS, and 100ul of infection medium was added to evaluate viral entry, while the mixed solutions of serially diluted antibodies in infection media were added to assess viral release. After 48h of incubation at 37°C, an HA assay was performed to detect the presence of the virus.

Neuraminidase (NA) assay. The NA assay was performed for all virus stocks. Microtiter 96-well plates (Immulon 4 HBX; Thermo Fisher Scientific) were coated with 25ug/ml (100ul/well) of fetuin (Sigma) diluted in coating solution (KPL) and incubated overnight at 4°C. The following day, clade 2.3.4.4b (H5N1-PR8) virus was serially diluted 1:2 in PBS containing 5% bovine serum albumin (blocking solution) in a separate 96-well plate, starting with the undiluted stock. Fetuin-coated plates from the previous day were washed three times with PBS-T and viral dilutions in 100ul were transferred to the fetuin-coated plates and incubated at 37°C for 6h. The plates were washed four times with PBS-T. Peanut agglutinin conjugated to HRP (PNA-HRP; Sigma) at a concentration of 5ug/ml diluted in PBS (100ul/well) was added, and the reaction mixture was incubated at RT for 1.5h. After incubation, the plates were washed again four times with PBS-T and developed for 10min with 100ul/well TMB (Thermo Scientific). The developing process was stopped with 50ul/well 3M hydrochloric acid, and the reaction was immediately read at an optical density (OD) of 490nm using a Synergy H1 hybrid multimode microplate reader (BioTek). To determine the optimal virus concentration to be used in the neuraminidase inhibition (NAI) assay, the absorbance data were plotted in GraphPad Prism 10. The data were fitted to a nonlinear regression curve to determine the 50% effective concentration (EC_{50}). The EC_{50} was subsequently used for NAI assays.

Neuraminidase inhibition assay. Microtiter 96-well plates (Immulon 4 HBX; Thermo Fisher Scientific) were coated with 25ug/ml (100ul/well) of fetuin (Sigma) diluted in coating solution (KPL) and incubated overnight at 4°C. The following day, anti-H5 mAbs were serially diluted in sample dilution at a starting concentration of 30ug/ml in duplicate. As a positive control anti-NA antibody, 1G01 was used, and as a negative control anti-SARS-CoV-2 spike antibody. The clade 2.3.4.4b (H5N1-PR8) virus was diluted in PBS at 2x the determined EC_{50}, in an NA-assay described previously. Fetuin-coated plates were washed with PBST, virus-antibody mixes, virus-only mixes, or medium only were added to the plates and incubated for 6h at 37°C. The plates were washed and incubated with 5ug/100ul/well of for 1.5h at RT. Plates were washed four times with PBS-T and developed for 10min with TMB. The developing process was stopped with 3M hydrochloric acid, and the reaction was immediately read at an optical density (OD) of 490nm using a Synergy H1 hybrid multimode microplate reader (BioTek). For all mAbs, half inhibitory concentration (IC_{50}) was calculated based on a dose-response curve, using top and bottom constraints of 0 and 100%, using GraphPad Prism 10.

NA-Star assay. The NA-Star Influenza Neuraminidase Inhibitor Resistance Detection Kit (Applied Biosystems) was used to evaluate whether the mAbs specifically target the neuraminidase enzymes' ability to cleave a small, soluble, chemiluminescent substrate. To assess antibody inhibition, mAbs were diluted 1:3 in NA-Star Assay Buffer at a starting concentration of 30ug/ml in a final volume of 25ul per well, in white 96-well cell culture plates. Next, 25ul of the clade 2.3.4.4b (H5N1-PR8) virus at the determined 2x EC_{50} concentration was added to each well, followed by shaking and a 30min incubation at 37°C. The rest of the assay was carried out in accordance to the manufacturer's instructions. Data points were expressed as percent inhibition of the maximum NA enzymatic activity, which was measured from the virus only wells. For all mAbs, the IC_{50} was calculated based on a dose-response curve, using top and bottom constraints of 0 and 100%, using GraphPad Prism 10.

Infectious virus determination via plaque assay. Briefly, 250ul of 10-fold dilutions of lung homogenates in PBS were used to infect the day before plated MDCK cells and incubated for lh at 37°C, testing each dilution in duplicate. Cells were then washed once with PBS and overlayed with oxoid agar (Oxoid), serum-free 2×MEM/bovine serum albumin (BSA) containing diethylaminoethanol (DEAE) dextran, supplemented with (TPCK)-treated trypsin. After 48h of incubation, cells were fixed using 4% formaldehyde and stained for H5 antigens. Plaque forming units were determined by staining with a well-defined anti-H5 mAbs primary antibody, followed by goat anti-human IgG (Fab specific)-peroxidase antibody (Sigma-Aldrich) and positive cells were visualized with the use of TrueBlue substrate (KPL-Seracare).

IgG digestion. Tris-ethylenediaminetetraacetic acid (EDTA), L-cysteine, and papain were combined at a final concentration of 100mM Tris, 2mM EDTA, 10mM L-cysteine, and 1mg/ml papain at 37°C for 15min to activate the enzyme. Purified IgG were incubated with activated papain at 37°C for 4-5h, using 40ul of activated papain per mg of IgG. Digestion was halted by adding iodoacetamide to a final concentration of 0.03M. 50-100ul of IgG Fc Capture Select (ThermoFisher) resin was washed with TBS and incubated with the digestion solution for 30min to 1h at RT to capture free Fc and undigested IgG. Resin was pelleted, and the supernatant was collected and concentrated using a 10kDa Amicon concentrator.

Immune complexing and negative stain EM. Monoclonal Fab and H5 (either A/Jiangsu/NJ210/2023 or A/Red-tailed Hawk/New York/NYCVH 22-8477/2022) were complexed at a 3:1 molar ratio for 1h at RT. To prepare nsEM grids, 3ul of immune complexes were applied to glow-discharged, carbon-coated 400 mesh copper grids at a concentration of ~10-20ug/m (Electron Microscopy Services). The Whatman filter paper was used to blot the excess sample, and 3ul of 2% w/v uranyl formate was applied to stain complexes for 60s twice. Samples were imaged on either a Talos 200C with a Falcon II direct electron detector and a CETA-16M camera (FEI) at 200 kV, 73,000 × magnification, and 2.00 Å/pixel; a Talos 200C with a Falcon II direct electron detector and a CETA 4k camera (FEI) at 200 kV, 73,000 × magnification, and 1.98 Å/pixel; or a Tecnai Spirit T12 (FEI) with a CMOS 4k camera (TVIPS) at 120 kV, 52,000 × magnification, and 2.06 Å/pixel. Micrographs were collected using Leginon. For each complex, 30k to 100k particles were picked and stacked using Appion and subsequently processed to generate 2D classes and 3D reconstructions using Relion 3.0 or Relion 4.0b1[5,6]. 3D reconstructions of A/Jiangsu/NJ210/2023 and A/Red-tailed Hawk/New York/NYCVH 22-8477/2022 complexes used initial reference models of 30 Å volumes generated from PDB 6E7G and 4K62, respectively. UCSF ChimeraX was used to generate composite 3D reconstructions[7].

CryoEM grid preparation and imaging. Fabs of 12G1 and 20D10 were incubated with Jiangsu H5 and CR9114[3] Fab at a 3:1:3 molar ratio for 1h at RT prior to cryoEM grid preparation and placed on ice until ready for use. Fabs of 1A1 and 6G1 were co-incubated with Jiangsu H5 and CR9114 at a molar ratio of 3:3:1:3. Prior to sample application, a PELCO easiGlow (Ted Pella Inc.) was used to plasma treat Quantifoil R1.2/1.3 Cu, 300-mesh grids (Quantifoil Micro Tools GmbH) for 25s at 15mA. A Vitrobot Mark IV (Thermo Fisher Scientific) was used to vitrify all samples at chamber temperature of 4°C, 100% humidity, blot force 1, wait time 5s, and blot times between 3-5s. To decrease orientation bias, immune complexes (~0.7-0.85mg/ml) were mixed with n-Octyl-beta-D-glucoside (OBG, Anatrace) to a final OBG concentration of 0.1% immediately before freezing. Grids were screened and datasets were collected on a 200kV Glacios (Thermo Fisher) equipped with a Falcon IV direct electron detector. For the 12G1 complex and the 1A1 + 6G1 co-complex, automated data collection was executed using EPU (Thermo Fisher) at 190,000× nominal magnification and a pixel size of 0.725 Å, with an approximate exposure dose of 45 e-/Å2 442 and a nominal defocus range of -0.7 to -1.4um. The 20D10 complex was collected similarly, but with a pixel size of 0.718. Each dataset contained ~2000-7000 movie micrographs.

Cryo-EM data processing. The CryoSPARC Live software was used for image preprocessing, which automatically performs image motion corrections and initial CTF estimations[8]. Further data processing with processed micrographs was then performed in CryoSPARC. Blob picker was used for initial particle picking. After particle extraction particles were subjected to several iterations of 2D classification and 2D class selection to remove junk particles. A final stack of particles was then subjected to Ab-Initio Reconstruction. The ab-initio classes were then used as reference models for a Heterogeneous Refinement job. Particles corresponding to 3D volumes with the best resolution and alignment were then subjected to Homogeneous Refinement. To overcome preferred orientation issues, particles corresponding to orientations that were overrepresented were removed using Rebalance Orientations, and the remaining particles were used for a Non-uniform Refinement job. In the case of 20D10, another iteration of the steps from Heterogeneous Refinement to Non-uniform Refinement were performed to end up with a rebalanced and well-aligning particle subset. In the case of 6G1, the non-uniform refined particles were used for a

Reference-Based Motion Correction job, after which the motion corrected particles were used for a second Non-uniform Refinement job. In all instances, non-uniform refined particles were symmetry expanded to the C3 axis in accordance with the trimeric nature of HA, and to maximize occupancy of the Fabs in the case of partial stoichiometry. The symmetry expanded particle set was then used for a 3D classification job using sphere masks around the epitope and Fab density. Highest-resolution and best-aligning classes were selected (in some cases aided by Regroup 3D Classes) and used for Local Refinement employing a soft solvent mask encompassing the HA trimer and the Fab. Following a Global CTF Refinement job, further Local Refinement was performed to obtain a high-resolution map. As the map of 20D10 still showed signs of orientation bias at this point, a Rebalance Orientations job followed by Local Refinement was performed to generate the final map.

Atomic model building. The initial model of HA H5 Jiangsu was kindly shared by Olivia Swanson while initial models of 6G1, 12G1 and 20D10 Fab were generated using ABodyBuilder 2.0. Initial models of HA and Fabs were fitted into the map density using ChimeraX after which the complex was further refined manually using Coot[7,9] Next several iterations of Real-space refinement in Phenix, followed by manual model building in Coot were performed to improve model statistics[10]. Model to map fit was validated using the integrated tools Molprobity and EMRinger in the Phenix software package. Orientations of all glycans were assessed and corrected using Privateer[11]. Due to diffuse density in the respective areas the following glycans/residues were not modeled: glycan N154 in the model of 20D10, glycan N154 in chain b in the model of 12G1, and residues 272 and 273 in chain A, B and C in the model of 6G1. Final atomic models were submitted to the Protein Data Bank with accession codes found in Table S1. Figures including atomic models were all produced using ChimeraX.

Biolayer-interferometry (BLI) assay. H5 conformational competition binding of antibodies from clonotype 1 and selected antibodies from clonotypes 2, 3, and 5 was assessed using a ForteBio Octet HTX (Sartorious). HIS-tagged H5 protein from clade 2.3.4.4b virus and the antibodies were diluted in kinetics buffer (1xPBS, 0.02% Tween 20, 0.1% BSA). First, Ni-NTA sensor tips were loaded with 100ug/ml of HIS-tagged H5 protein for 300 seconds (s) to achieve a binding shift at ~1nm. After loading of antigen, tips were transferred to wells containing 50ug/ml of capture antibody for 300s with >600nm binding to ensure complete blocking of the antigen epitopes. Sensors were then transferred to wells containing secondary antibodies (detection antibody) 10ug/ml for 300s. We tested two antibodies from clonotype 1 (1A1, 13E8) to verify the observed pattern; one antibody from clonotype 2 (20D10), a different epitope binding antibody to clonotype 1, and an irrelevant anti-SARS antibody, here used as a control. An observable binding response at this stage indicated non-competition as compared to irrelevant control (SARS), while a lack of response or a reduction of response indicated competition. Data were analyzed using Sartorius Octet biolayer interferometry analysis software, version 12.2.13.5

Supplementary Figures

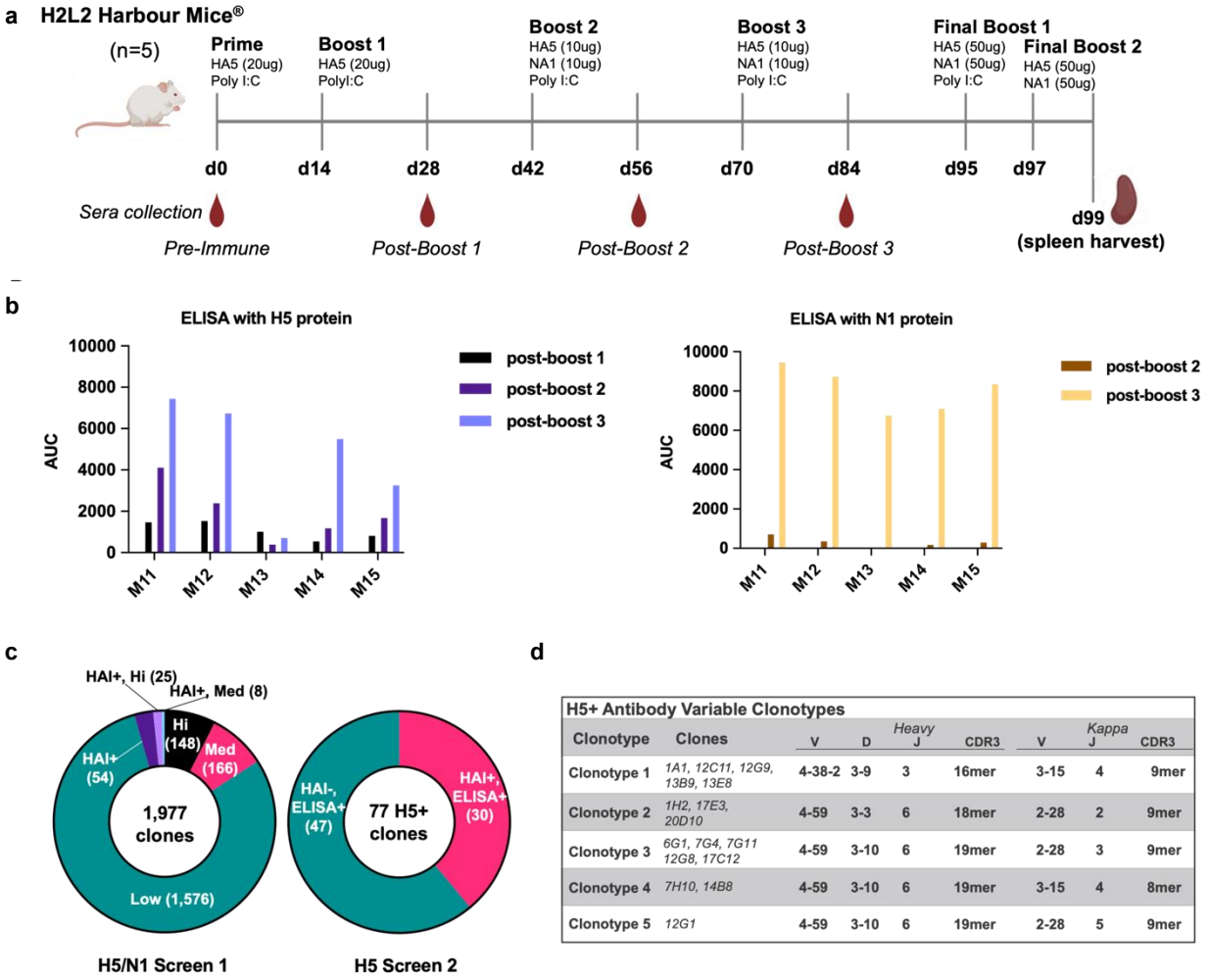

H5+ Antibody Variable Clonotypes

Clonotype	Clones	Heavy V	Heavy D	Heavy J	Heavy CDR3	Kappa V	Kappa J	Kappa CDR3
Clonotype 1	*1A1, 12C11, 12G9, 13B9, 13E8*	4-38-2	3-9	3	16mer	3-15	4	9mer
Clonotype 2	*1H2, 17E3, 20D10*	4-59	3-3	6	18mer	2-28	2	9mer
Clonotype 3	*6G1, 7G4, 7G11 12G8, 17C12*	4-59	3-10	6	19mer	2-28	3	9mer
Clonotype 4	*7H10, 14B8*	4-59	3-10	6	19mer	3-15	4	8mer
Clonotype 5	*12G1*	4-59	3-10	6	19mer	2-28	5	9mer

Supplementary Fig. 1. Immunization in H2L2 Harbour Mice® with HA and NA protein of H5N1 clade 2.3.4.4b virus. a The timeline for vaccination is shown in the upper panel. Five female H2L2 Harbour Mice® were immunized by intraperitoneal injection with the protein amounts shown in the figure, adjuvanted with poly I:C. Serum was collected at the indicated time points, and the final immunization was performed two and four days before the spleen was harvested for hybridoma fusion (created with BioRender.com). **b** Collected sera were tested against the H5 (left) and N1 (right) proteins by enzyme-linked immunosorbent assay (ELISA). Based on the results, a single mouse was selected and sacrificed for spleen harvest and hybridoma fusion. In this graph, the x-axis represents the individual mice, and the y-axis represents the area under the curve (AUC) for the response with the sera. The AUC was calculated using GraphPad Prism 10, with the average plus three standard deviations of the blank wells serving as the baseline. **c** A total of 1,977 hybridoma clones were generated from the top responding mouse. Supernatants from the clones were first screened by ELISA coated with a combination of H5 and N1 proteins. Hemagglutinin inhibition (HI) assays were also performed at a fixed supernatant dilution of 1:10. ELISA binders were compared to a 1:100 dilution of unimmunized sera (normal mouse sera, NMS) and were classified as high (Hi) (>3x NMS), medium (Med) (1.5-3x NMS), and low (<1.5x NMS), with and without HI activity (right pie graph). All medium and high binding clones with and

without HI activity were down-selected for secondary screening (401 clones) by H5-specific ELISAs and HI assays. Seventy-seven total clones (30%) rescreened positive by either ELISA or HI (left pie graph). The top thirty clones that were both ELISA and HI positive were down-selected for isotyping, variable segment sequencing and recombinant production as human G1/ kappa. **d** Clonotype analysis based on shared complementarity-determining region 3 (CDR3) sequence (shared length and >90% amino acid identity) and shared VDJ/ VJ gene usage on the sequences of the top performing sixteen clones revealed five closely related clonotypes. Source data are provided as a Source Data file.

Supplementary Fig. 2. Phylogenetic analysis of the HA sequence of the viruses used throughout the study. The phylogenetic tree here was constructed using the HA amino acid (aa) sequence of H5N1 viruses isolated from infected birds and mammals, including humans. Color coded in purple are: the H5N1 virus used as the antigen, A/mallard/New York/22-008760-007-original/2022; the H5N1 virus strains obtained from the New York City Virus Hunters (NYCVH): A/chicken/New York/NYCVH 168127/2023, A/Canada goose/New York/NYCVH 23-453/2023, A/Canada goose/New York/NYCVH 22-9190/2022, A/peregrine falcon/New York/NYCVH 160820/2022, and A/red-tailed hawk/New York/NYCVH 22-8477/2022, the H5N1 virus strain used for cell culture assays, A/bald eagle/FL/W22-134-OP/2022; finally, H5N8 and H5N2 virus strains isolated in 2014 from two different geographic locations: A/chicken/Netherlands/14015531/2014 and A/Northern pintail/Washington/40964/2014, respectively. Color coded in orange, is the recently detected H5N1 bovine virus: A/dairy cattle/Texas/24-008749-001-original/2024. Color coded in blue are virus strains isolated from humans infected with H5N1 virus strains from 2005 to 2023: A/Vietnam/1203/2004 (H5N1), A/Indonesia/5/2005 (H5N1), A/Shenzhen/1/2016 (H5N6), A/Cambodia/NPH230032_2/2023 (H5N1), A/Jiangsu/NJ210/2023 (H5N1) and virus strains isolated from humans infected with H1N1 virus A/Wisconsin/67/2022. The scale represents a 0.02% difference in amino acid sequence.

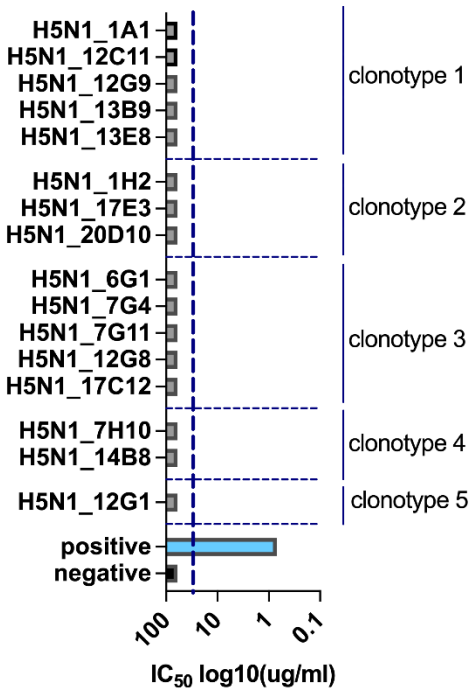

Supplementary Fig. 3. Neuraminidase inhibition of mAbs via direct binding to the enzyme's active site. MAbs capacity to inhibit enzymatic activity of NA protein of clade 2.3.4.4b virus was tested in duplicates, with a positive control an anti-NA antibody, 1G01[12]. Data shown as half inhibitory concentration (IC_{50}) (ug/ml). Negative control for all the assays was an anti-SARS-CoV-2 spike antibody[4]. Source data are provided as a Source Data file.

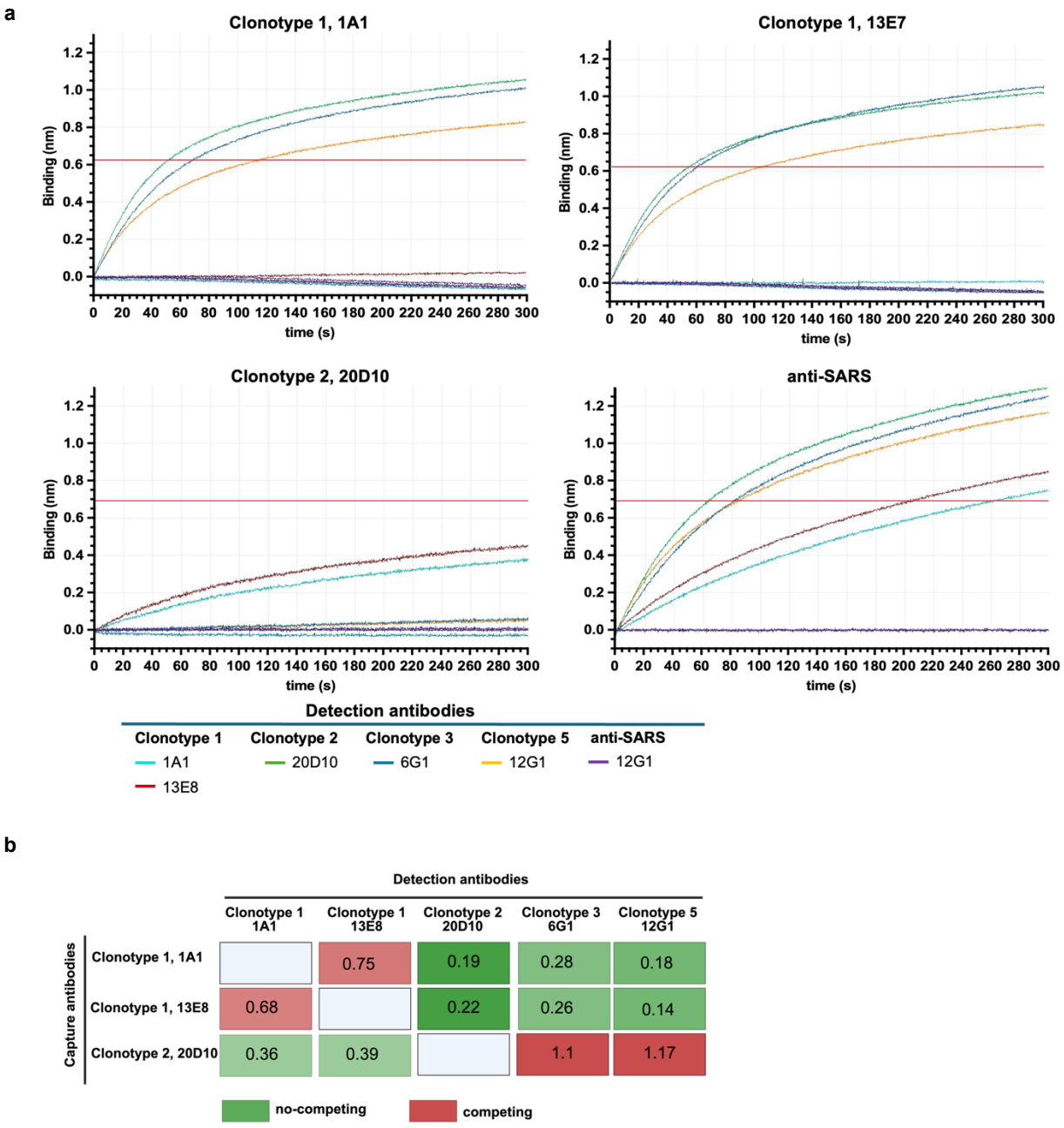

Supplementary Fig. 4. Binding properties of clonotype 1 and 2-5 anti-H5 mAbs. a The obtained curves with the use of the detection antibodies are plotted against the capture antibody, names, which are shown at the top of each graph. **b** Competition matrix of four anti-H5 mAbs. Each box displays the wavelength shift at 405nm for a specific mAb pair; values from anti-SARS control antibody were subtracted, representing negative binding of the detection mAb. Competing pairs are highlighted in red, while non-competing pairs are shown in green. Source data are provided as a Source Data file.

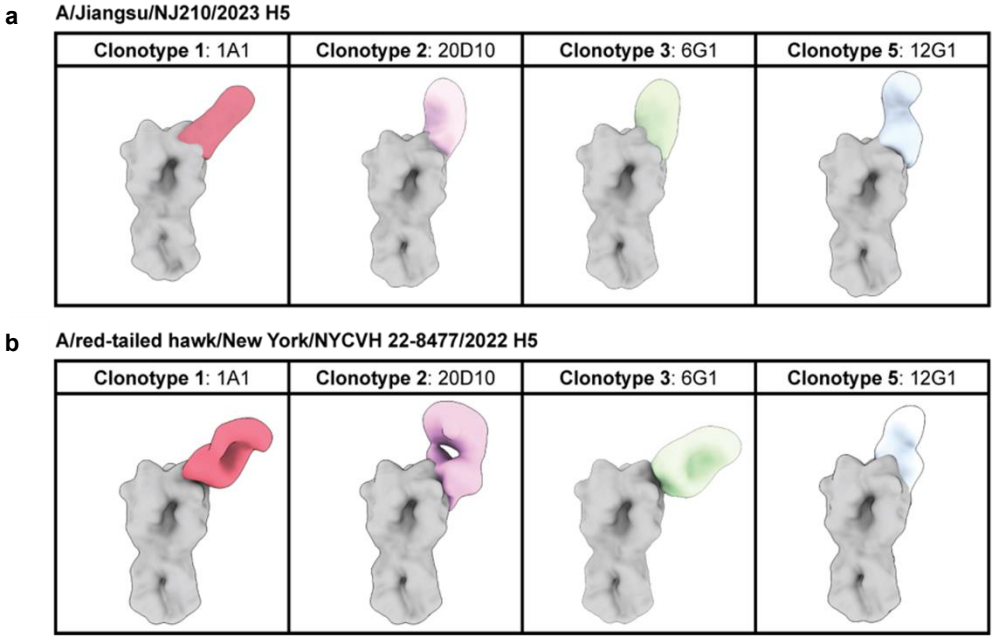

Supplementary Fig. 5. Negative stain EM reconstructions of representative mAbs for clonotypes 1-3 and 5. Maps demonstrate binding to either recombinant **a** A/Jiangsu/NJ210/2023 H5 or **b** A/red-tailed hawk/New York/NYCVH 22-8477/2022 H5 depicted on a map of A/Vietnam/1203/2004 H5 (PDB:6E7G) generated using ChimeraX.

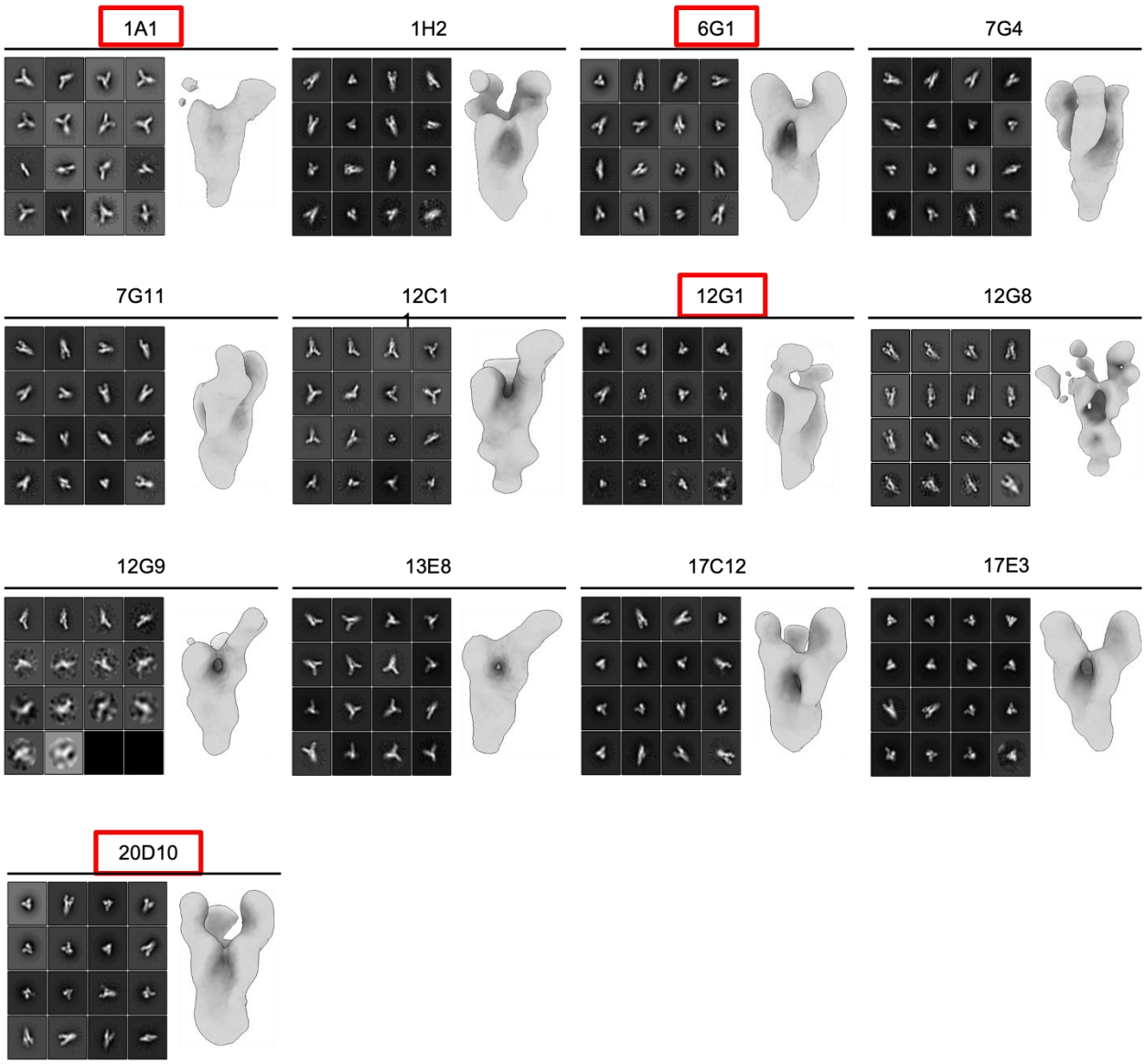

Supplementary Fig. 6. Negative stain EM representative 2D classes and 3D reconstructions of monoclonal antibodies bound to A/Jiangsu/NJ210/2023 H5. 2D class averages (left panels) representing particles used for negative stain 3D reconstructions (right panels) of mAbs in complex with recombinant A/Jiangsu/NJ210/2023 H5. Reconstructions were generated using Relion 3.0. mAbs selected as representative of their respective clonotypes and used for cryoEM analysis are boxed in red.

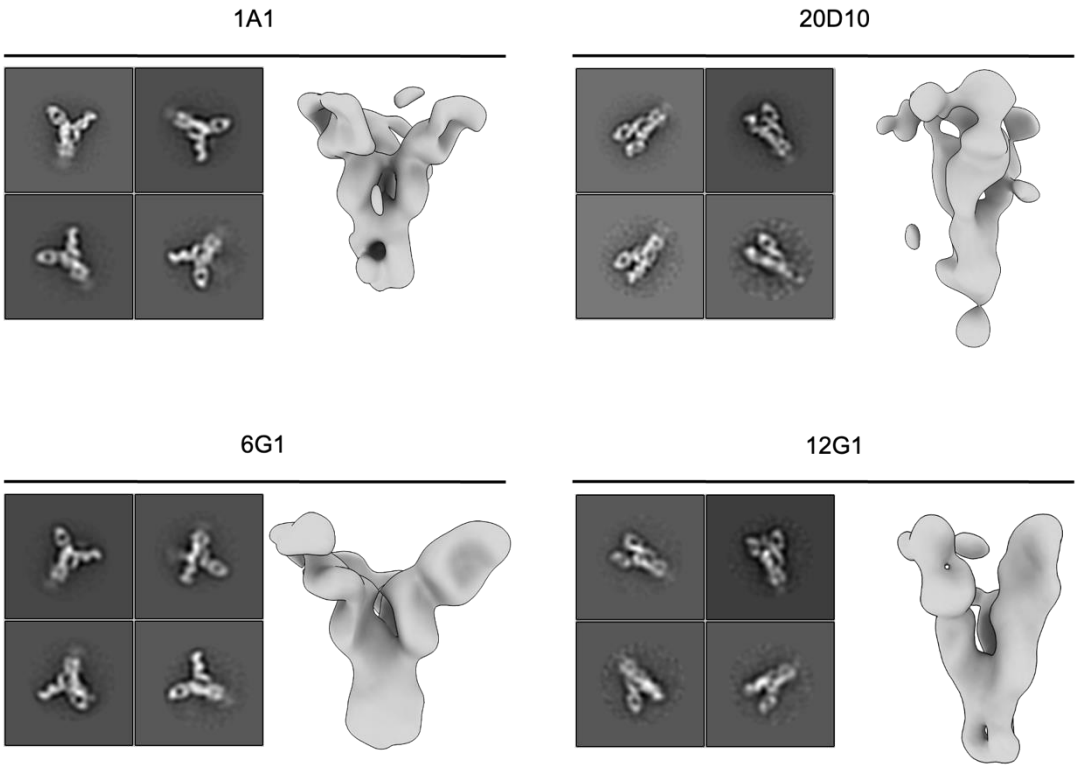

Supplementary Fig. 7. Negative stain EM representative 2D classes and 3D reconstructions of monoclonal antibodies bound to A/red-tailed hawk/New York/NYCVH 22-8477/2022 H5. 2D class averages (left panels) representing particles incorporated in negative stain 3D reconstructions (right panels) of mAbs in complex with recombinant A/Jiangsu/NJ210/2023 H5. Reconstructions were generated using Relion 3.0.

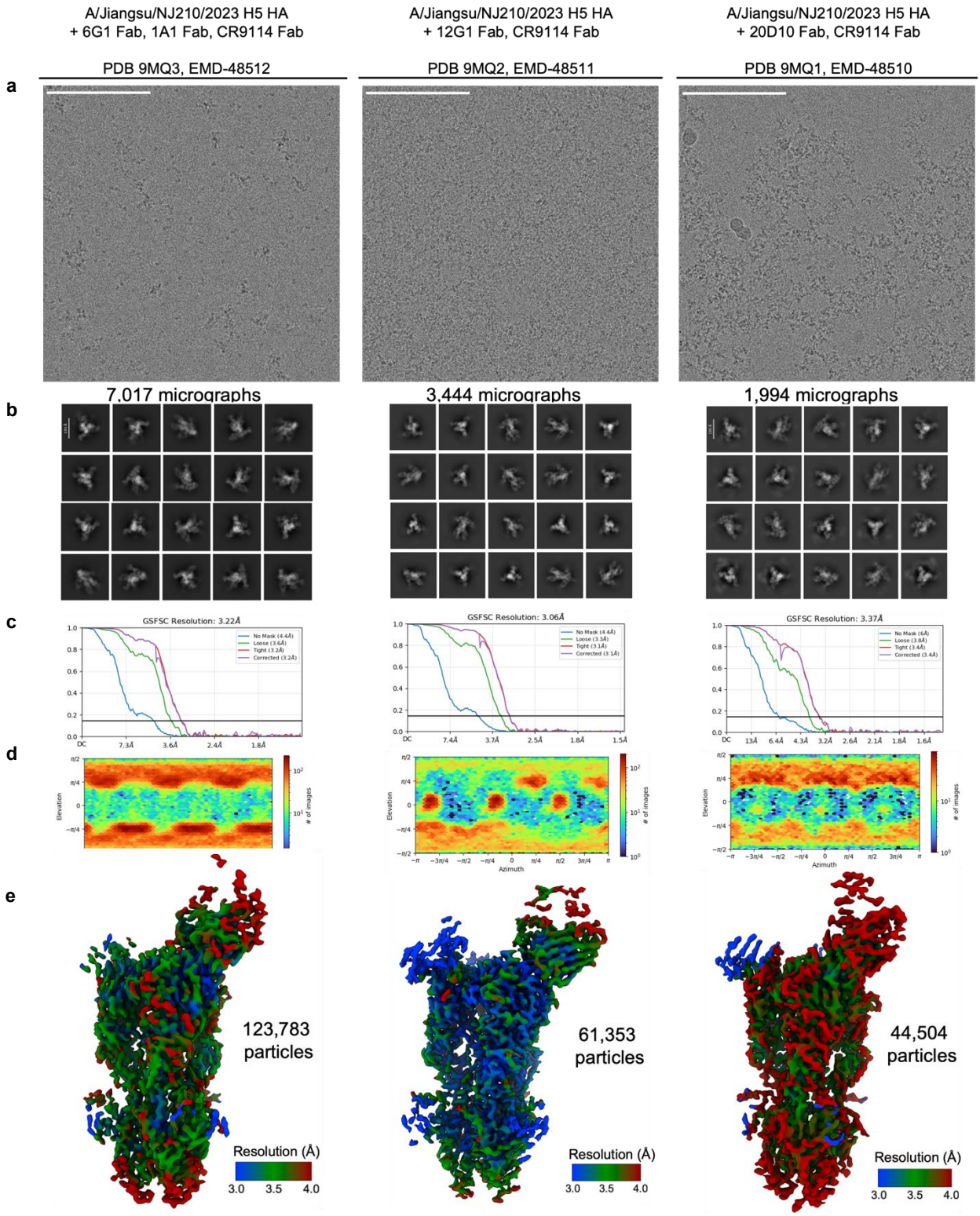

Supplementary Fig. 8. CryoEM workflow. a Representative micrographs with 100nm white scale bars. **b** Top 20 classes of final 2D class average selection after 2D clean up steps. **c** Fourier shell correlation (FSC) plots, **d** Viewing distribution plots, **e** Local resolution maps and particle count for final 3D reconstructions.

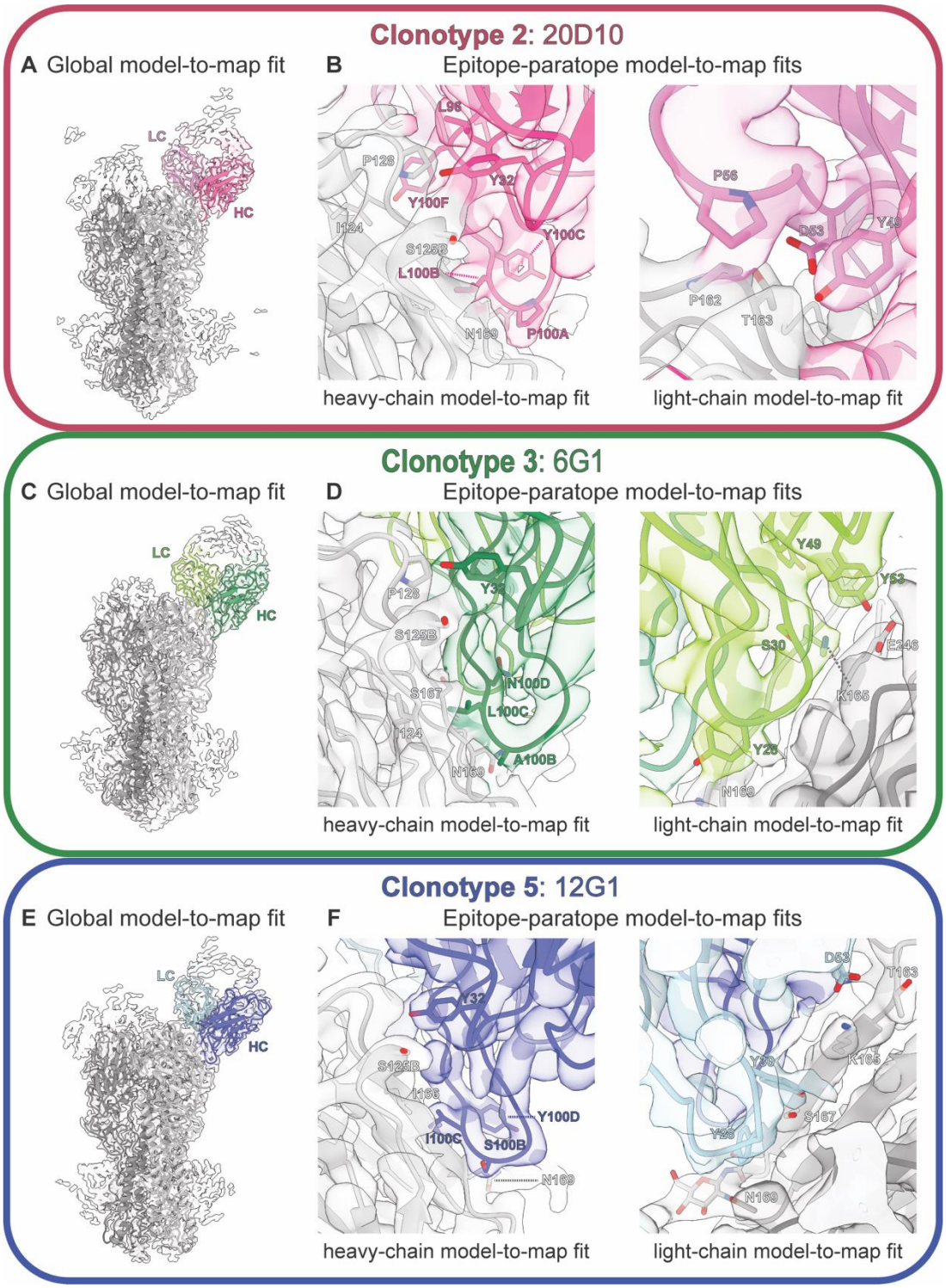

Supplementary Fig. 9. CryoEM model-to-map fit. Final PDB models docked into their corresponding EM maps. Both global fits and epitope-paratope fits are presented. **a-b** Global and local fits for clonotype 1. **c-d** Analogous model-to-map fits for clonotype 3. **e-f** Analogous model-to-map fits for clonotype 5.

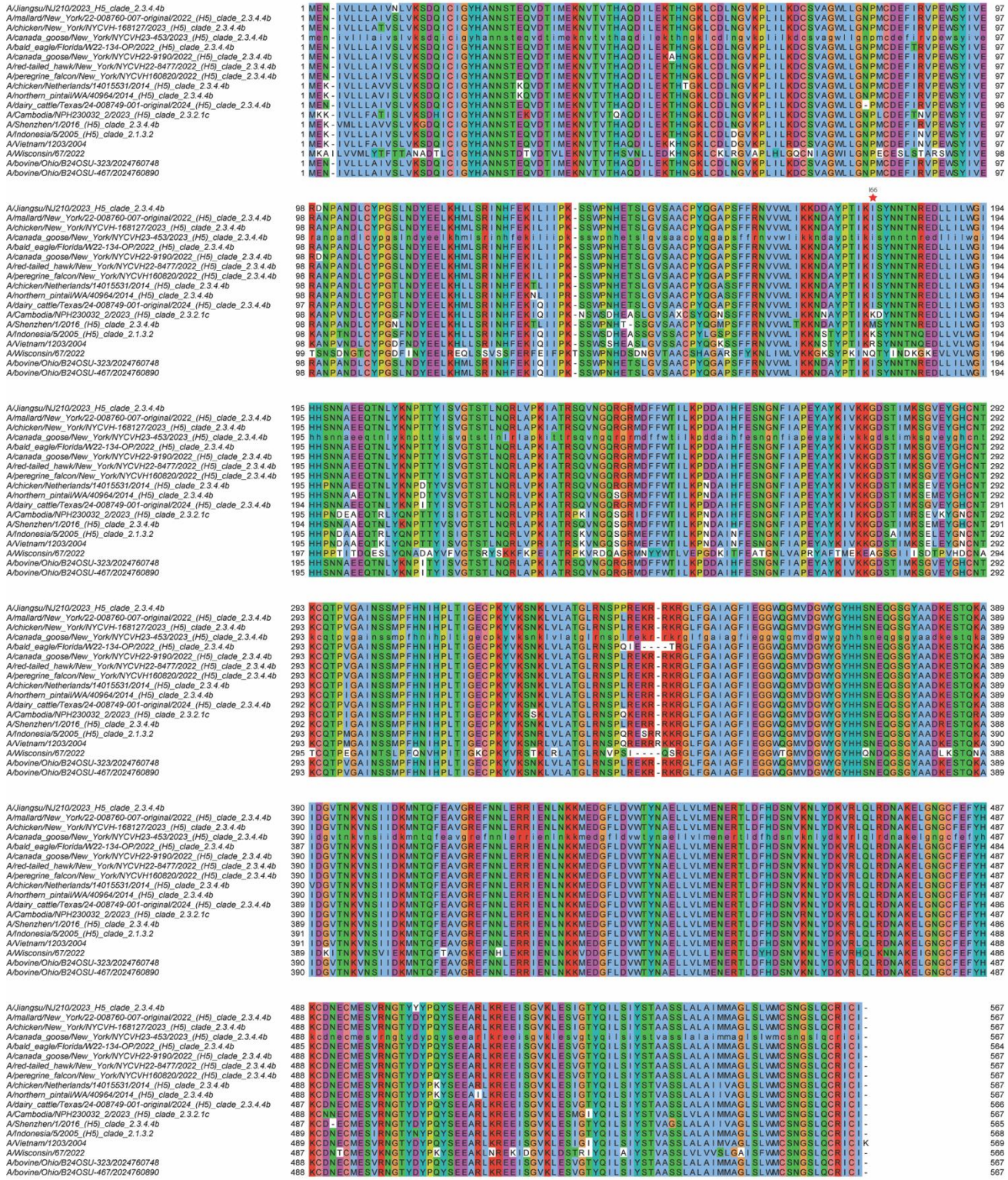

Supplementary Fig. 10. Multiple sequence alignment in H5 numbering. ClustalW alignment of all HA proteins used in this study, including the panel of clade 2.3.4.4b H5 sequences used to

generate Fig. 5e. Alignments are presented in H5 numbering. Residue I266 is identified with a red star above the column of interest.

Supplementary Table 1. Cryo-EM data collection, processing, model refinement and validation statistics.

	H5 + 6G1	H5 + 12G1	H5 + 20D10
Access codes			
PDB	9MQ3	9MQ2	9MQ1
EMDB	EMD-48512	EMD-48511	EMD-48510
Data collection and processing			
Microscope	Glacios	Glacios II	Glacios
Magnification			
Voltage (kV)	200	200	200
Electron exposure ($e^-/Å^2$)	42.39	44.85	44.74
Defocus range (μm)			
Pixel size (Å)	0.725	0.718	0.725
Imposed Symmetry	C1	C1	C1
Final particle number	123,783 (post symmetry-expansion)	61,353 (post symmetry-expansion)	44,504 (post symmetry-expansion)
Map resolution (Å)	3.22	3.06	3.37
FSC Threshold	0.143	0.143	0.143
Map sharpening B-factor ($Å^2$)	-79.5	-59.2	-64.5
Model refinement and validation			
Total Residues	1688	1660	1689
Amino-acids	1673	1640	1677
Carbohydrates	15	20	12
RMSD Bonds	0.005	0.005	0.006
RMSD Angles	0.890	0.830	0.967
Ramachandran			
Outliers (%)	0	0	0
Allowed (%)	4.66	4.19	4.03
Favored (%)	95.34	95.81	95.97
Rotamer outliers (%)	0	0	0
Clash score	4.07	3.48	2.26
Molprobity score	1.52	1.43	1.28
FSC model (0/0.143/0.5)	3.0/3.2/3.7	2.9/3.0/3.3	3.2/3.3/3.9
EMRinger score	3.11	3.47	2.30

Supplementary Table 2. Contacts between monoclonal antibodies and A/Jiangsu/NJ210/2023 H5.

Clonotype 2: 20D10			
HC	**H5 Jiangsu Pos**	**Chain**	**Interaction**
31	125B	A	VDW
32	125B	A	HBSB. VDW
32	128	A	VDW
96	128	A	HP, VDW
101	129	A	VDW
100A	168	A	VDW
100A	169	A	HBBB, VDW
100B	123	A	VDW
100B	124	A	HP, VDW
100B	125	A	VDW
100B	168	A	VDW
100C	167	A	HBBB, VDW
100C	169	A	VDW
100D	126	A	VDW
100F	129	A	VDW
100F	164	A	HBSB. VDW
LC	**H5 Jiangsu Pos**	**Chain**	**Interaction**
56	129	A	VDW
54	162	A	VDW
56	162	A	HP, VDW
49	163	A	HBSB, VDW
53	163	A	HBSS, VDW
30	165	A	VDW
50	165	A	VDW
53	165	A	VDW
28	167	A	VDW
30	167	A	VDW
28	244	A	VDW
30	244	A	VDW
30	246	A	VDW
LC	**H5 Jiangsu Pos**	**Chain**	**Interaction**
67	187	B	VDW
67	189	B	VDW
30	219	B	VDW
27C	227	B	VDW
27E	227	B	HBSB, VDW
28	227	B	HBSB, VDW
29	227	B	VDW

Clonotype 3: 6G1			
HC	**H5 Jiangsu Pos**	**Chain**	**Interaction**
31	125B	A	VDW
32	125B	A	HBSB, VDW
96	128	A	HP, VDW
101	128	A	VDW
101	129	A	VDW
100B	168	A	VDW
100B	169	A	HBBB, VDW
100B	171	A	VDW
100C	123	A	VDW
100C	124	A	HP, VDW
100C	168	A	VDW
100D	167	A	HBBB, VDW
100E	126	A	VDW
100E	165	A	VDW
100E	166	A	VDW
100G	128	A	VDW
100G	163	A	VDW
100G	166	A	VDW
LC	**H5 Jiangsu Pos**	**Chain**	**Interaction**
57	160	A	VDW
49	162	A	VDW
56	162	A	VDW
49	163	A	HBSB, VDW
30	165	A	HBSS, VDW
50	165	A	VDW
28	167	A	VDW
28	169	A	HBSS, VDW
28	242	A	VDW
28	244	A	VDW
53	246	A	HBSS, VDW
28	323	A	VDW
LC	**H5 Jiangsu Pos**	**Chain**	**Interaction**
67	187	B	HBSS, VDW
67	189	B	VDW
28	219	B	VDW
29	219	B	VDW
27E	227	B	VDW
28	227	B	HBSB, VDW
29	227	B	VDW

Clonotype 5: 12G1			
HC	**H5 Jiangsu Pos**	**Chain**	**Interaction**
32	125B	B	HBBB, VDW
96	128	B	VDW
100A	171	B	VDW
100B	168	B	VDW
100B	169	B	HBBB, VDW
100B	171	B	VDW
100C	166	B	HP, VDW
100C	168	B	VDW
100D	167	B	HBBB, VDW
100E	126	B	VDW
100E	166	B	VDW
100G	128	B	VDW
LC	**H5 Jiangsu Pos**	**Chain**	**Interaction**
56	129	B	HBSS, VDW
49	163	B	HBSB, VDW
53	163	B	VDW
52	165	B	HBSS, VDW
53	165	B	HBSS, VDW
30	167	B	HBSS, VDW
28	169	B	HBSS, VDW
28	242	B	VDW
28	244	B	VDW
28	323	B	HBLS, VDW
LC	**H5 Jiangsu Pos**	**Chain**	**Interaction**
28	219	C	VDW
27E	222	C	VDW
27C	227	C	VDW
27E	227	C	HBSB, VDW
29	227	C	VDW

The getcontacts program (https://getcontacts.github.io/index.html) was used on final models of 20D10, 6G1, and 12G1 in complex with A/Jiangsu/NJ210/2023 H5 to predict protein-protein interactions between amino acid residues. Relevant interactions are abbreviated as follows: van der Waals (VDW), side-chain to backbone hydrogen bonding (HBSB), backbone to backbone hydrogen bonding (HBBB), side-chain to side-chain hydrogen bonding (HBSS), and hydrophobic (HP). Source data are provided as a Source Data file.

References

1 Meade, P. S. *et al.* Detection of clade 2.3.4.4b highly pathogenic H5N1 influenza virus in New York City. *J Virol* **98**, e0062624 (2024). https://doi.org:10.1128/jvi.00626-24

2 Marizzi, C. & Wright, L. Hunting emerging viruses through participatory community science. *Nat Microbiol* **9**, 578-581 (2024). https://doi.org:10.1038/s41564-024-01604-1

3 Dreyfus, C. *et al.* Highly conserved protective epitopes on influenza B viruses. *Science* **337**, 1343-1348 (2012). https://doi.org:10.1126/science.1222908

4 Clark, J. J. *et al.* Protective effect and molecular mechanisms of human non-neutralizing cross-reactive spike antibodies elicited by SARS-CoV-2 mRNA vaccination. *Cell Rep* **43**, 114922 (2024). https://doi.org:10.1016/j.celrep.2024.114922

5 Lander, G. C. *et al.* Appion: an integrated, database-driven pipeline to facilitate EM image processing. *J Struct Biol* **166**, 95-102 (2009). https://doi.org:10.1016/j.jsb.2009.01.002

6 Kimanius, D., Dong, L., Sharov, G., Nakane, T. & Scheres, S. H. W. New tools for automated cryo-EM single-particle analysis in RELION-4.0. *Biochem J* **478**, 4169-4185 (2021). https://doi.org:10.1042/BCJ20210708

7 Pettersen, E. F. *et al.* UCSF ChimeraX: Structure visualization for researchers, educators, and developers. *Protein Sci* **30**, 70-82 (2021). https://doi.org:10.1002/pro.3943

8 Punjani, A., Rubinstein, J. L., Fleet, D. J. & Brubaker, M. A. cryoSPARC: algorithms for rapid unsupervised cryo-EM structure determination. *Nat Methods* **14**, 290-296 (2017). https://doi.org:10.1038/nmeth.4169

9 Emsley, P. & Cowtan, K. Coot: model-building tools for molecular graphics. *Acta Crystallogr D Biol Crystallogr* **60**, 2126-2132 (2004). https://doi.org:10.1107/S0907444904019158

10 Liebschner, D. *et al.* Macromolecular structure determination using X-rays, neutrons and electrons: recent developments in Phenix. *Acta Crystallogr D Struct Biol* **75**, 861-877 (2019). https://doi.org:10.1107/S2059798319011471

11 Agirre, J. *et al.* Privateer: software for the conformational validation of carbohydrate structures. *Nat Struct Mol Biol* **22**, 833-834 (2015). https://doi.org:10.1038/nsmb.3115

12 Stadlbauer, D. *et al.* Antibodies targeting the neuraminidase active site inhibit influenza H3N2 viruses with an S245N glycosylation site. *Nat Commun* **13**, 7864 (2022). https://doi.org:10.1038/s41467-022-35586-7